CARBON 50 (2012) 201–208

Available at www.sciencedirect.com

SciVerse ScienceDirect

journal homepage: www.elsevier.com/locate/carbon

Thickness-dependent azobenzene doping in mono- and few-layer graphene

Namphung Peimyoo [a], *Ting Yu* [a,b,*], *Jingzhi Shang* [a], *Chunxiao Cong* [a], *Huanping Yang* [a]

[a] *Division of Physics and Applied Physics, School of Physical and Mathematical Sciences, Nanyang Technological University, 637371 Singapore, Singapore*

[b] *Department of Physics, Faculty of Science, National University of Singapore, 117542 Singapore, Singapore*

ARTICLE INFO

Article history:
Received 28 June 2011
Accepted 17 August 2011
Available online 24 August 2011

ABSTRACT

Doping effects on exfoliated graphenes induced by methyl orange (MO) have been studied by spatially resolved Raman spectroscopy. When the MO molecules were adsorbed on the top of graphenes, the charge transfer between them caused two outcomes simultaneously. One is the strong chemical doping in graphenes and the other is the enhanced Raman signals of MO molecules. Our finding provides a potential approach for manipulating the electronic properties of graphenes and investigating the vibrational properties of molecules. Moreover, the thickness-dependent doping effects in graphenes are unambiguous distinguished by Raman imaging. The possible origin was discussed and designated to the different band structures of graphenes and the screening effect.

1. Introduction

Chemical doping of graphenes has attracted a great deal of interest because of their unique ability to adapt the electronic structures of graphenes. Previously, surface adsorption and intercalation of dopant species were used to obtain chemically doped graphenes. Charge transfer between metals and graphene can occur when their work functions are different [1]. Charges may immigrate from graphenes to metals if work functions of metals are higher than that of graphene or vice versa. For organic adsorbates, charge transfer between graphene and organic molecules is normally driven by the difference between electron affinity or ionization energy of organic molecules and work function of graphene. One potential effect of charge transfer is change of the electrical environment of graphene such as inducing a positive (p-doping) or a negative (n-doping) electrical potential. Another possible phenomenon is the chemical enhancement of molecular Raman signals [2]. In recent, several dopant species [3,4] have demonstrated their capabilities in doping graphene. On one side, some inorganic materials, such as Au, Ag, Br or I, have been found to induce different doping effects for mono-, bi- and tri-layer graphenes, being related to the strong interaction between metals and monolayer graphene [5,6] or the screening effect [4]. On the other side, organic molecules perform more promising prospects [7,8] owing to high doping efficiency, stable morphology and high controllability. Up to now, there are some experiments on doping monolayer graphene with organic molecules [7–9]. For the potential application for adjusting the electronic properties of graphenes, doping effects of organic molecules on different graphene layers are expected to be explored. However, only few studies [10,11] were reported on this topic.

Among organic molecules, azobenzene mainly comprises of two aromatic benzene rings connected with N=N, has been extensively reported on many applications such as photoswitching [12] and reversible optical memory storage [13]. Recently, Zhang et al. studied on functionalization of graphene oxide with azobenzene moieties and observed the change of graphene oxide conductance [14]. Considering the azobenzene

* *Corresponding author at:* Division of Physics and Applied Physics, School of Physical and Mathematical Sciences, Nanyang Technological University, 637371 Singapore, Singapore.
E-mail address: yuting@ntu.edu.sg (T. Yu).
0008-6223/$ - see front matter
doi:10.1016/j.carbon.2011.08.035

molecules consisting of aromatic rings, electron donating and/or electron accepting groups, we hypothesize that azobenzene can stably attach on graphene via π–π interaction and is able to induce doping effects.

In this work, we decorate graphenes with one of azobenzene derivatives: methyl orange (MO), through surface absorption. Doping effects of MO on graphenes and MO Raman signals have been studied. The systematic Raman mapping and spectroscopy analysis clearly reveal thickness dependence of doping effects and enhanced Raman signals of MO. We propose that the thickness dependence of doping is due to the difference of band structures and screening effects in graphenes. Both factors result in the doping level of monolayer graphene is higher than those of thick graphenes.

2. Materials and methods

Graphenes were peeled off from the highly ordered pyrolytic graphite (HOPG) by using the adhesive tape [15] and then transferred onto a SiO_2/Si wafer. Pristine graphenes and MO modified graphenes (MO/graphenes) were characterized by Raman spectroscopy, optical microscopy, and atomic force microscopy (AFM). It is worth noting that Raman spectroscopy has been proved to be an excellent tool for studying graphene [16], as it can be used efficiently for identifying the number of layers [17,18], distinguishing the type of doping [19–21], probing strain [22], providing the defect information [23,24], probing the electronic structure of graphene [17,25] and identifying the edge orientations [26] and stacking orders [27]. Here, the number of graphene layers was determined by Raman spectroscopy according to the G band intensity and the 2D band width. MO was dissolved in the dimethylformamide (DMF) solution with three different concentrations: 2×10^{-3}, 2×10^{-5} and 2×10^{-7} M. After that, MO molecules were anchored on graphene by spin coating and rinsing with the distilled water to remove unadsorbed molecules.

Raman spectra and Raman images of pristine graphenes and MO/graphenes were collected using a WITEC CRM200 Raman system with a 532 nm excitation laser. The laser spot is about 0.5 μm in diameter. A 100× objective lens with NA = 0.95 was used. The incident laser power was operated below 0.3 mW to avoid damages of molecule and thermal effects

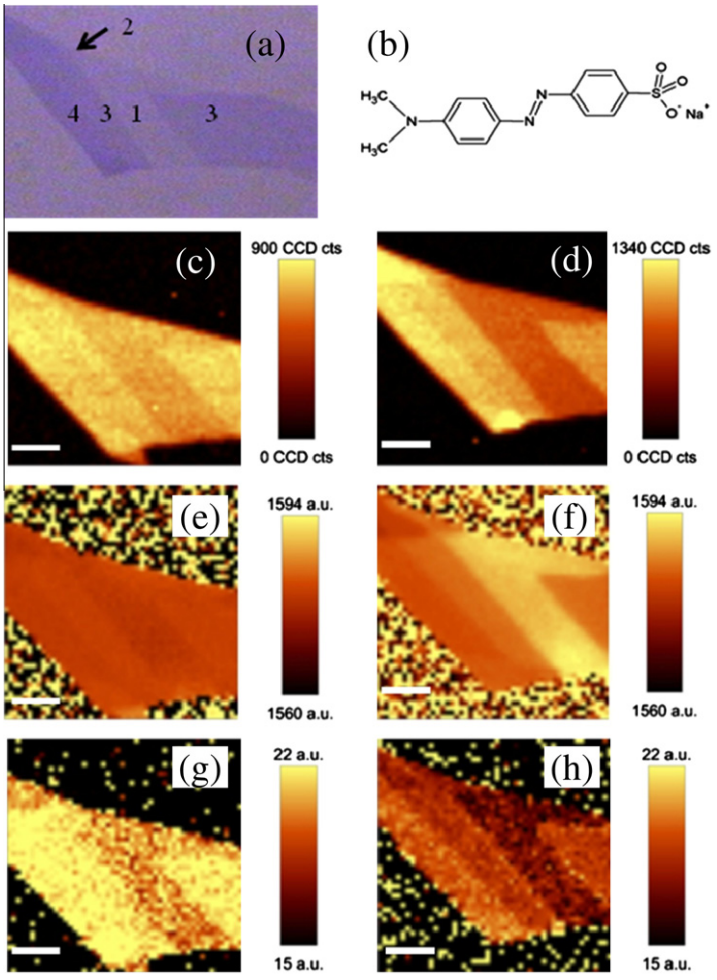

Fig. 1 – (a) Optical image of graphenes including monolayer (1 L), bilayer (2 L), trilayer (3 L) and tetralayer (4 L) as denoted. (b) The chemical structure of Methyl Orange (MO). (c–h) Raman images of graphenes before (left column) and after (right column) MO deposition at the concentration of 2.0×10^{-5} M. (c, d) Raman images of 2D band intensities. (e, f) Raman images of G band positions. (g, h) Raman images of G band full-width at half-maximum (FWHM). The scale bars are 3 μm in length.

caused by laser. The exposure time of 0.5 s was used for obtaining Raman images, while the Raman spectra were collected using exposure time of 60 s. In addition, Si band at 520 cm^{-1} was used for calibration.

3. Results and discussion

The graphenes consisting of 1–4 layers (L) in the same pieces were selected for Raman measurements. In order to study thickness-dependent doping effects and the uniformity of molecule adsorbed on graphenes, Raman mapping of samples before and after modification was performed (Fig. 1). The number of layers can be distinguished by reading the integrated intensity of the G band (I_G) (Fig. S1a), the 2D (or G′) width [17,18,24] (Fig. S1b) and the contrast spectrum [28] (Fig. S1c and d). The Raman images of the integrated intensity of 2D band (I_{2D}) before and after modification can be seen in Fig. 1c and d. The I_{2D} images of the sample with molecular deposition show the obvious thickness dependence: monolayer ($I_{2D/1L}$) > bilayer ($I_{2D/2L}$) > trilayer ($I_{2D/3L}$) > tetralayer ($I_{2D/4L}$). Fig. 2 shows the typical Raman spectra of graphenes before and after MO modification. The prominent feature in this figure is that the relative intensities between the 2D and G bands (I_{2D}/I_G) reduce after modification for all number of layers, which suggests the existence of doping [21].

After modification, several MO bands were observed in the range between 1050 and 1630 cm^{-1} as shown in the inset of Fig. 2a. The band at 1158 cm^{-1} labeled as M_1 is attributed to the stretching mode of C–S or C–C, the weak peak at 1290 cm^{-1} is ascribed to the stretching mode of C–N, denoted as M_2 and the most intense band at ~1500 cm^{-1} is originated from the stretching mode of N-aromatic ring, named as M_3 [29]. The presence of the strong intensity of M_3 band supports that the parallel alignment of molecule with respect to graphene surface is favorable. The disorder-related D band appears at ~1350 cm^{-1} in the MO/graphenes, which implies an increase of the disorder in the graphene basal plane caused by MO. Raman spectroscopic analysis stands for the MO molecules adsorbed on graphenes through π–π interaction.

Furthermore, two strong molecular bands denoted as M_1 and M_3 were selected for Raman images as shown in Fig. 3a and b, respectively. The Raman images of MO show the perfect correspondence with G band image of graphenes (Fig. S1a). More interestingly, the M_3 signal presents the thickness-dependent behavior: its strongest signal appears in 1 L graphene and the M_3 intensity decreases gradually for thick graphenes (Fig. 3b). By contrast, it should be mentioned that the molecular bands on the SiO_2/Si substrate were not detectable. Our observation indicates that graphene is a favorable substrate for enhancing MO molecular Raman signals. Furthermore, when increasing the MO concentration to 2.0×10^{-3} M, the thickness dependences of the intensities of both M_1 and M_3 bands were found as shown in Fig. 3c and d, respectively.

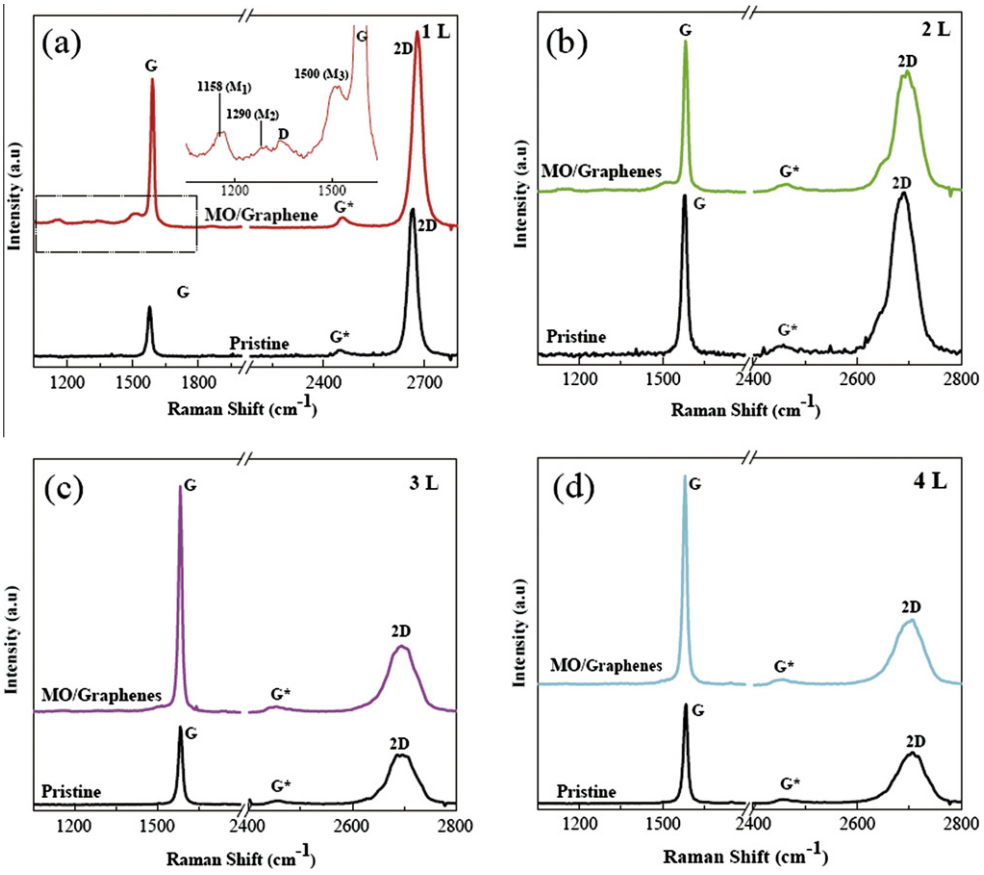

Fig. 2 – Raman spectra of graphenes before and after molecular deposition. (a) 1 L (b) 2 L (c) 3 L and (d) 4 L graphenes. The inset of (a) shows the molecular bands enhanced by 1 L graphene. The graphene sample was modified by a MO solution with concentration of 2.0×10^{-5} M.

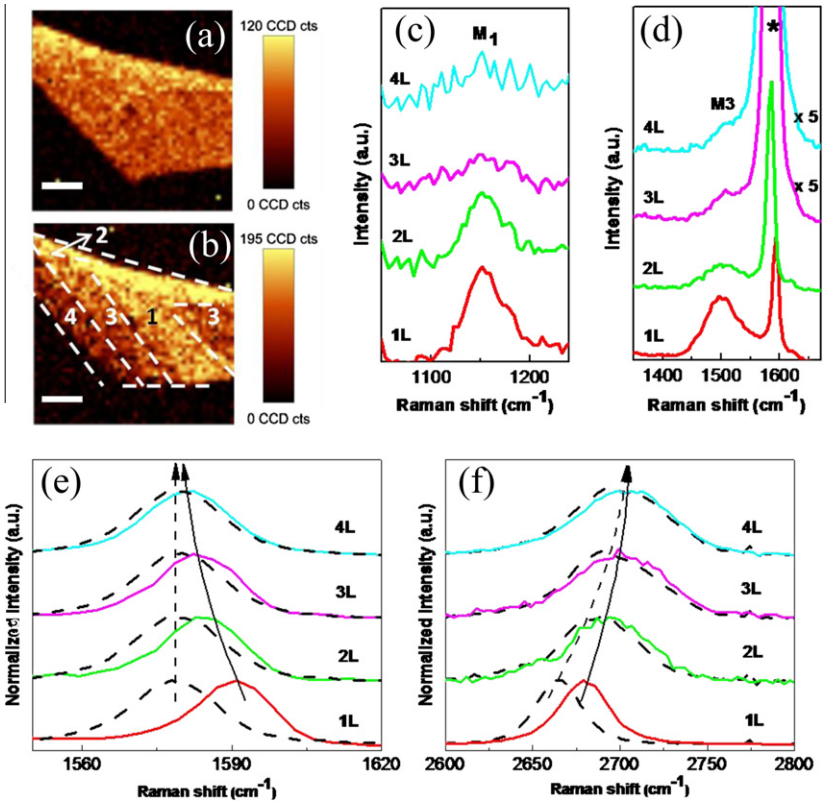

Fig. 3 – Raman images of the M_1 (a) and M_3 (b) band intensity of MO. The scale bars are 3 μm in length. Raman spectra of M_1 (c) and M_3 (d) bands for different number of layers. The peak labeled by the star (*) is the graphene G band. The molecular signals are normalized by setting the intensity of Si peak at 520 cm^{-1} as one. (e) Raman spectra of G bands from pristine graphenes (dashed line) and MO/graphenes (solid line) with different number of layers. (f) Raman spectra of 2D bands from pristine graphenes (dashed line) and MO/graphenes (solid line). To compare the peak positions, the G and 2D band intensities have been normalized to one. The MO concentrations are 2.0×10^{-5} M and 2.0×10^{-3} M for (a, b, e, f) and (c, d), respectively.

As illustrated in Fig. 3e and f, MO/graphenes show obvious thickness-dependent doping effects. The center of G and 2D bands (fitted by a single Lorentzian) are also indicated (dashed and solid arrows). The Raman G bands of the pristine samples were observed at ~1580 cm^{-1} for all layers which is a fingerprint of neutral or undoped graphenes [20,21]. After introducing the MO molecule onto the graphenes, the G band positions shift towards higher frequency (blue-shift) but the blue-shift decreases with the thickness of graphenes. Similarly, thickness dependences of the G band positions were reported on Ag/graphenes and Au/graphenes [5,6].

Regarding the thickness dependence of molecular Raman signal enhancement on the number of graphene layers mentioned above, one possibility might be due to the molecules absorbed differently on graphenes, another is the different charge transfer efficiency between graphenes and molecules [2]. The adsorbed molecules on graphenes were confirmed by height profiles of the selected lines on AFM images of 1 L graphene before (Fig. 4a) and after MO modification (Fig. 4b). First, it can be clearly seen that the roughness obviously increases after modification (Fig. 4d). Second, if the molecular film was deposited on graphenes homogeneously, the height difference crossing along two different layers should be integer time/times of the thickness of one graphene layer. The height difference in the cross section along 3 L and 4 L graphenes (Fig. 4e) is 0.37 nm, very close to the thickness of 1 L pristine graphene and the height difference along 1 L and 3 L graphenes of ~0.70 nm (Fig. 4f) corresponds to the thickness of 2 L pristine graphenes. Hence, it can be concluded that MO molecules were uniformly distributed on various thickness graphenes. In comparison, we prefer the different charge transfer efficiency contributing to the thickness-dependent enhancement of MO Raman signals.

The statistical data including the full-width at half-maximum (FWHM), the positions of G and 2D bands and the I_{2D}/I_G of pristine graphenes and modified graphenes with MO concentration of 2×10^{-5} M are presented in Fig. 5. With the increasing number of layers, the shifts of G band of the MO/graphenes decrease (Fig. 5a). In details, the position of G band increases ~12 cm^{-1} for 1 L, ~5 cm^{-1} for 2 L, ~4 cm^{-1} for 3 L and ~2 cm^{-1} for 4 L graphenes, respectively. Fig. 5b shows the narrowing of FWHM of G band as a function of the number of layers in MO/graphenes. The FWHMs (G) for 1–4 L graphene are ~17 cm^{-1}, ~17.8 cm^{-1}, ~18.6 cm^{-1} and ~19.5 cm^{-1}, respectively. The widths of G bands in pristine 1–4 L graphenes are almost identical, being ~21 ± 1 cm^{-1}. Here, the stiffening of G band is owing to the non-adiabatic removal of the Kohn anomaly, a softening of G phonons near the Γ point [20]. The sharpening of G band is caused by the blockage of the decay channel of phonons into electron–hole pairs due to the Pauli

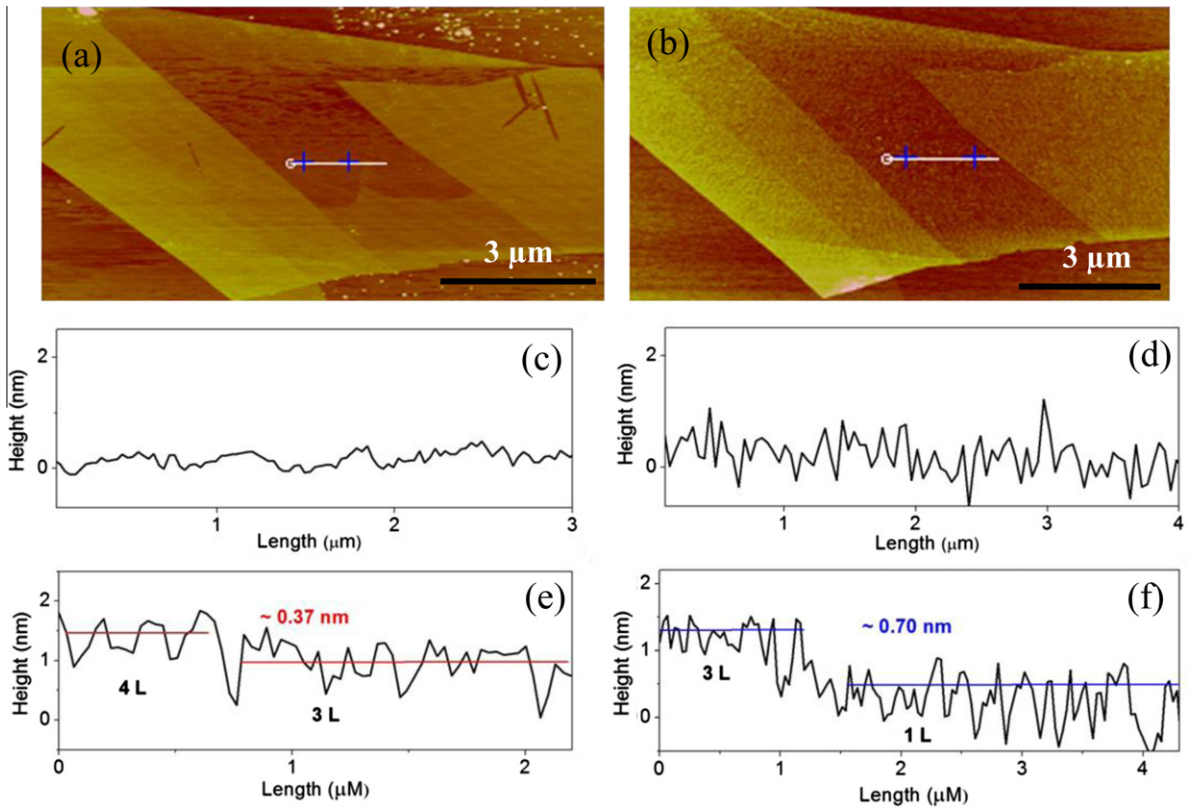

Fig. 4 – AFM images before (a) and after (b) MO deposition. (c, d) Height profiles of selected lines on 1 L graphene in (a) and (b), respectively, showing the increased surface roughness after molecular modification. (The graphene sample was coated by a MO solution with concentration of 2.0×10^{-5} M.) (e) Cross section along 3 L and 4 L modified graphenes. The different height, ~0.37 nm is close to the thickness of 1 L pristine graphene. (f) Cross section along 1 L and 3 L graphenes. The different height, ~0.70 nm agrees well with the thickness of 2 L pristine graphenes.

exclusion principle and consequently the increasing phonon life time [20]. The decrease of FWHM will saturate when a shift of Fermi level caused by doping is bigger than half of phonon energy [19,20].

In Fig. 5c, the 2D band positions of MO doped graphenes shift to higher frequencies and the 2D position shift of 1 L graphene is larger than those of few layer graphenes, being similar to G band. The shifts of the G and 2D bands can be used to identify the type of doping [20,21]. The blue shifts of both G and 2D bands indicate the existence of p doping, whereas the blue-shift of G band and red-shift of 2D band indicate n-doping. In our case, the graphene sample is p-doped induced by MO molecule (see Table S1 in Supplementary Data for details of the widths and positions of G and 2D bands), where electrons are transferred from graphenes to MO molecules.

The variation of I_{2D}/I_G of graphene sample before and after modification is shown in Fig. 5d. I_{2D}/I_G is sensitive to the doping effects and its reduction is consistent with the existence of either p- or n-doping [21]. Clearly, the reduction of I_{2D}/I_G before and after modification decreases significantly with the increasing thickness. That indicates the doping level in 1 L > 2 L > 3 L > 4 L. The cause of reduction is from the decrease of the 2D band integrated intensity, owing to an increase of the electron–electron interactions [30]. The similar decreases of the ratio were reported on doping of 1 L graphene with aromatic molecules [8], diazonium salt [9], tetrathiafulvalene (TTF) and tetracyanoethylene (TCNE) [31], various benzene molecules [32]. By comparing the shift of the G band position with those studies [8,31,32] at the similar concentrations, MO molecules cause a stronger doping in graphenes.

For the thickness-dependent doping, we propose it need to be understood by combining two kinds of viewpoints: one is the difference of band structures of graphenes and the other is the screening effect. According to the electrically gated experiment in 1 L and 2 L graphene, the change of G band position of 1 L graphene to doping level is more sensitive than that of bilayer graphene [30,33]. This was attributed to the difference of band structure of bilayer graphene, including two conduction and two valence sub-bands. The coupling between two graphene layers lead to parabolic dispersion and a large density of state near band touching point comparing to that of 1 L graphene [34]. These cause strong G phonon softening in 2 L graphene [34]. Thus the difference of band structure could be one reason that the doping in 2 L graphene is weaker than that in 1 L graphene. The trend can be expected up to 4 L graphene based on the current observation. Another possible reason of thickness-dependent doping is screening effect. The holes from the molecule are transferred to graphenes. According to theoretical calculation [35], those charges can be distributed uniformly on 1 L and 2 L graphene. Screening effect plays an important role when the graphene

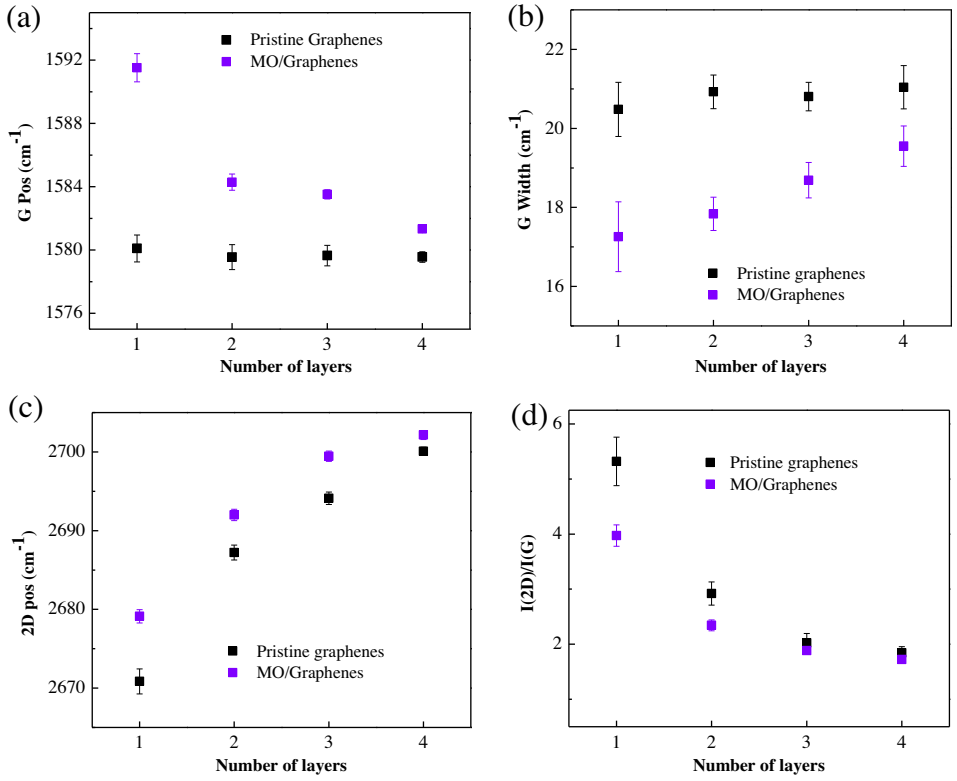

Fig. 5 – G band positions (a) and widths (b) of graphenes before and after molecular modification as a function of number of layers. (c) 2D band positions of graphenes before and after molecular modification. (d) Variation of the ratio of 2D and G band intensities before and after introducing the MO as a function of number of layers.

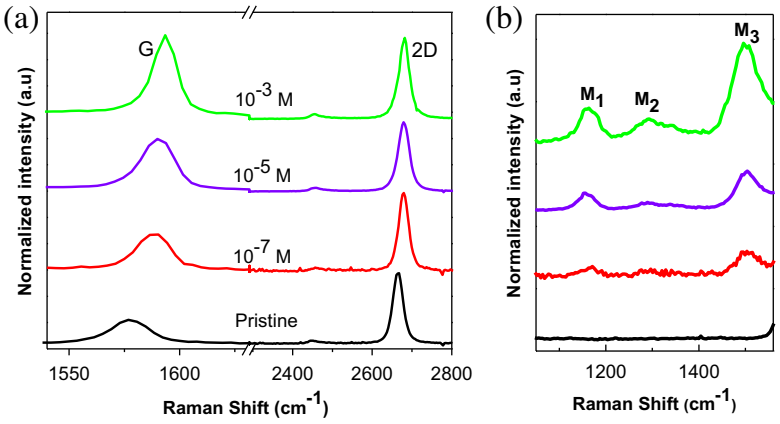

Fig. 6 – (a) Raman spectra of 1 L graphene before and after MO modification at different concentrations: 2×10^{-3}, 2.0×10^{-5} and 2.0×10^{-7} M. (b) Raman spectra of 1 L graphene modified with different solution concentrations, showing the molecular signals in the range 1050–1560 cm^{-1}. The intensities of the bands are normalized to the 2D intensity of 1 L pristine graphene.

sheet is thicker than 2 L (screening length) [35,36]. For graphenes thicker than the screening length, the charges are accumulated heavily on the surface layers leading to doping decays from the surface layers to interior layers [35]. This could be the reason that 2 L graphene is doped more heavily than 3 L graphene which is doped more than 4 L graphene.

Further, the influence of MO concentration on the doping effects and the chemical enhancement were investigated. Raman spectroscopic data of 1 L graphene before and after modification with three different MO concentrations are shown in Fig. 6a. With the increasing MO concentration, we can see the gradual decrease of I_{2D}/I_G, and the increases of the amounts of G band stiffening and narrowing. In Fig. 6b, the molecular band positions for graphenes modified with different concentrations from 2.0×10^{-3} to 2.0×10^{-7} M are identical. With the increase in the concentration, the intensity of Raman signals of molecules increases. Surprisingly, the molecular signals on graphenes are sufficient to be detected for the concentration as low as 2.0×10^{-7} M (see Supplementary Data Fig. S3).

The effects of MO concentration on the position and the FWHM of G band can be explained by the degrees of MO coverage. For the MO concentration of 2.0×10^{-5} M, the film thickness is ~0.3 nm as an evidence from the AFM image in Fig. S2a (see Supplementary Data), where the coverage of molecules is thought to be monolayer referring to the previous reports [2,37]. The coverage of lower concentration: 2.0×10^{-7} M can be considered to be submonolayer [2]. Referring to the shift and the narrowing of G band, the highest doping was found in the graphene samples doped by MO with concentration of 2.0×10^{-3} M because its degree of coverage was higher than monolayer. Indeed, the thickness of MO film can be up to three to four molecular layers when the MO solution of 2.0×10^{-3} M was used (see Supplementary Data Fig. S2b and d). When increasing the MO concentration higher than 2.0×10^{-3} M, there is no further blue-shift of G band (the result is not shown here). This saturation of doping is because the films are thicker at higher concentration so that those upper molecules do not cause the doping. In other words, when the distance between the upper molecules and the underlying graphene is beyond the critical value for the effective charge transfer, the contribution of upper MO molecules to doping is negligible. Based on our results, this critical value is 3–4 molecular layers in MO/graphenes.

4. Conclusions

Strong doping effects on graphenes with azobenzene molecule have been studied by Raman spectroscopy. The blue shifts of both G and 2D bands indicate that the graphenes are p-doped after MO modification. The charge transfer between MO and graphenes accounts for the chemical doping of graphenes and the enhanced Raman signal of MO. Raman features from the MO/graphenes show thickness-dependent phenomena, such as G band position, 2D band position, FWHM (G) and I_{2D}/I_G. The doping level is found to be highest in 1 L graphene and decreases with the number of graphene layers. Both band structure and screening effects take responsibilities for the thickness-dependent doping. Raman signals from MO also are related to the thicknesses of graphenes and the strongest MO signal is observed in 1 L graphene after modification, which corresponds to the most efficient charge transfer. The thickness influence of molecular film on doping of 1 L graphene and MO Raman signals was also investigated by adjusting the used MO concentrations. The saturation of doping in 1 L graphene was determined and the critical value for the charge transfer is estimated to be 3–4 molecular layers. Strikingly, the molecular Raman signals on graphenes can be monitored even when the used MO concentration is as low as 2.0×10^{-7} M. We believe that the understanding of thickness-dependent effects of MO/graphenes is essential for modifying the electronic properties of graphenes and potential applications, for example, a graphene-based biosensor for examining the organic molecules.

Acknowledgments

This work is supported by the Singapore National Research Foundation under NRF RF award No. NRF-RF2010-07 and MOE Tier 2 MOE2009-T2-1-037.

Appendix A. Supplementary data

Supplementary data associated with this article can be found, in the online version, at doi:10.1016/j.carbon.2011.08.035.

REFERENCES

[1] Giovannetti G, Khomyakov PA, Brocks G, Karpan VM, Brink J, Kelly PJ. Doping graphene with metal contacts. Phys Rev Lett 2008;101(2):026803.
[2] Ling X, Xie LM, Fang Y, Xu H, Zhang HL, Kong J, et al. Can graphene be used as a substrate for Raman enhancement? Nano Lett 2010;10(2):553–61.
[3] Chen JH, Jang C, Adam S, Fuhrer MS, Williams ED, Ishigami M. Charge impurity scattering in graphene. Nat Phys 2008;4:377–81.
[4] Jung N, Kim N, Jockusch S, Turro NJ, Kim P, Brus L. Charge transfer chemical doping of few layer graphenes: charge distribution and band gap formation. Nano Lett 2009;9(12):4133–7.
[5] Lee J, Novoselov KS, Shin HS. Interaction between metal and graphene: dependence on the layer number of graphene. ACS Nano 2011;5(1):608–12.
[6] Lee J, Shim S, Kim B, Shin HS. Surface-enhanced Raman scattering of single- and few-layer graphene by the deposition of gold nanoparticles. Chem Eur J 2011;17(8):2381–7.
[7] Chen W, Chen S, Qi DC, Gao XU, Wee ATS. Surface transfer p-type doping of epitaxial graphene. J Am Chem Soc 2007;129(34):10418–22.
[8] Dong X, Fu D, Fang W, Shi Y, Chen P, Li LJ. Doping single-layer graphene with aromatic molecules. Small 2009;5(12):1422–6.
[9] Farmer DB, Golizadeh-Mojarad R, Perebeinos V, Lin YM, Tulevski GS, Tsang JC, et al. Chemical doping and electron–hole conduction asymmetry in graphene devices. Nano Lett 2009;9(1):388–92.
[10] Sharma R, Baik JH, Perera CJ, Strano MS. Anomalously large reactivity of single graphene layers and edges toward electron transfer chemistries. Nano Lett 2010;10(2):398–405.
[11] Koehler FM, Jacobsen A, Ensslin K, Stampfer C, Stark WJ. Selective chemical modification of graphene surfaces: distinction between single- and bilayer graphene. Small 2010;6(10):1125–30.
[12] Evan SD, Johnson SR, Ringdorf H, Williams LM, Wolf H. Photoswitching of azobenzene derivatives formed on planar and colloidal gold surface. Langmuir 1998;14(22):6436–40.
[13] Hagen R, Bieringer T. Photoaddressable polymers for optical data storage. Adv Mater 2001;13(23):1805–10.
[14] Zhang X, Feng Y, Huang D, Li Y, Feng W. Investigation of optical modulated conductance effects based on a graphene oxide-azobenzene hybrid. Carbon 2010;48(11):3236–41.
[15] Novoselov KS, Geim AK, Morozov SV, Jiang D, Zhang Y, Dubonos SV, et al. Electric field effect in atomically thin carbon films. Science 2004;306(5696):666–9.
[16] Ni ZH, Wang YY, Yu T, Shen ZX. Raman spectroscopy and imaging of graphene. Nano Res 2008;1(4):273–91.
[17] Ferrari AC, Meyer JC, Scardaci V, Casiraghi C, Lazzeri M, Mauri F, et al. Raman spectrum of graphene and graphene layers. Phys Rev Lett 2006;97(18):187401.
[18] Gupta A, Chen G, Joshi P, Tadigadapa S, Eklund PC. Raman scattering from high-frequency phonons in supported n-graphene layer films. Nano Lett 2006;6(12):2667–73.
[19] Yan J, Zhang Y, Kim P, Pinczuk A, Electric field effect tuning of electron–phonon coupling in graphene. Phys Rev Lett 2007;98(16):166802.

[20] Pisana S, Lazzeri M, Casiraghi C, Novoselov KS, Geim AK, Ferrari AC, et al. Breakdown of the adiabatic Born–Oppenheimer approximation in graphene. Nat Mater 2007;6:198–201.
[21] Das A, Pisana S, Chakraborty B, Piscanec S, Saha SK, Waghmare UV, et al. Monitoring dopants by Raman scattering in an electrochemically top-gated graphene transistor. Nat Nanotechnol 2008;3:210–5.
[22] Yu T, Ni ZH, Du C, You YM, Wang YY. Shen, ZX. Raman mapping investigation of graphene on transparent flexible substrate: the strain effect. J Phys Chem C 2008;112(33):12602–5.
[23] Casiraghi C, Hartschuh A, Qian H, Piscanec S, Georgi C, Fasoli A, et al. Raman spectroscopy of graphene edges. Nano Lett 2009;9(4):1433–41.
[24] Ferrari AC. Raman spectroscopy of graphene and graphite: disorder, electron–phonon coupling, doping and nonadiabatic effects. Solid State Commun 2007;143:47–57.
[25] Malard LM, Nilsson J, Elias DC, Brant JC, Plentz F, Alves ES, et al. Probing the electronic structure of bilayer graphene by Raman scattering. Phys Rev B 2007;76(20):201401.
[26] Cong CX, Yu T, Wang HM. Raman study on the G mode of graphene for determination of edge orientation. ACS Nano 2010;4(6):3175–80.
[27] Cong CX, Yu T, Saito R, Dresselhaus GF, Dresselhaus MS. Second-order overtone and combination Raman modes of graphene layers in the range of 1690–2150 cm^{-1}. ACS Nano 2011;5(5):1600–5.
[28] Ni ZH, Wang HM, Kasim J, Fan HM, Yu T, Wu YH, et al. Graphene thickness determination using reflection and contrast spectroscopy. Nano Lett 2007;7(9):2758–63.
[29] Zhang A, Fang Y. Influence of adsorption orientation of methyl orange on silver colloids by Raman and fluorescence spectroscopy: pH effect. Chem Phys 2006;331(1):55–60.
[30] Basko DM, Piscanec S, Ferrari AC. Electron–electron interactions and doping dependence of the two-phonon Raman intensity in graphene. Phys Rev B 2009;80(16):165413.
[31] Voggu R, Das B, Rout CS, Rao CNR. Effects of charge transfer interaction of graphene with electron donor and acceptor molecules examined using Raman spectroscopy and cognate techniques. J Phys: Condens Matter 2008;20(47):472204.
[32] Das B, Voggu R, Rout CS, Rao CNR. Changes in the electronic structure and properties of graphene induced by molecular charge-transfer. Chem Commun 2008;41:5155–7.
[33] Das A, Chakraborty B, Piscanec S, Pisana S, Sood AK, Ferrari AC. Phonon renormalization in doped bilayer graphene. Phys Rev B 2009;79(15):155417.
[34] Yan J, Henriksen EA, Kim P, Pinczuk A. Observation of anomalous phonon softening in bilayer graphene. Phys Rev Lett 2008;101(13):136804.
[35] Guinea F. Charge distribution and screening in layered graphene systems. Phys Rev B 2007;75(23):235433.
[36] Ziegler D, Gava P, Güttinger J, Moliter F, Wirtz L, Lazzeri M, et al. Variations in the work function of doped single- and few-layer graphene assessed by Kelvin probe force microscopy and density functional theory. Phys Rev B 2011;83(23):235434.
[37] Gorgoi M, Michaelis W, Kampen TU, Schlettwein D, Zahn DRT. Thickness dependence of the LUMO position for Phthalocyanines on hydrogen passivated silicon (111). Appl Surf Sci 2004;234:138–43.